

# The challenge of unravelling magnetic properties in LaFeAsO

I.I. Mazin and M.D. Johannes

*Code 6693, Naval Research Laboratory, Washington, DC 20375*

L. Boeri

*Max-Planck-Institut für Festkörperforschung, Heisenbergstrasse 1, D-70569 Stuttgart, Germany*

K. Koepernik

*IFW Dresden, P.O. Box 270116, D-01171 Dresden, Germany*

D.J. Singh

*Materials Science and Technology Division, Oak Ridge National Laboratory, Oak Ridge, Tennessee 37831-6114*

(Dated: February 2, 2022)

First principles calculations of magnetic and, to a lesser extent, electronic properties of the novel LaFeAsO-based superconductors show substantial apparent controversy, as opposed to most weakly or strongly correlated materials. Not only do different reports disagree about quantitative values, there is also a schism in terms of interpreting the basic physics of the magnetic interactions in this system. In this paper, we present a systematic analysis using four different first principles methods and show that while there is an unusual sensitivity to computational details, well-converged full-potential all-electron results are fully consistent among themselves. What makes results so sensitive and the system so different from simple local magnetic moments interacting via basic superexchange mechanisms is the itinerant character of the calculated magnetic ground state, where very soft magnetic moments and long-range interactions are characterized by a particular structure in the reciprocal (as opposed to real) space. Therefore, unravelling the magnetic interactions in their full richness remains a challenging, but utterly important task.

PACS numbers:

The discovery of high temperature superconductivity in LaFeAsO<sub>1-x</sub>F<sub>x</sub> by Kamihara and co-workers<sup>1</sup> rising to critical temperatures  $T_c$  over 50K with rare earth substitution,<sup>2</sup> has resulted in a great deal of experimental<sup>2,3,4,5,6,7,8,9,10,11,12</sup> and theoretical activity.<sup>13,14,15,16,17,18,19,20,21,22,23,24,25,26,27,28,29</sup> These studies have shown that this set of Fe-based superconductors displays a remarkably rich set of physical properties. Besides the high critical temperatures, which include the highest known values of  $T_c$  outside the cuprates, there is evidence for several types of Fermi surface nesting<sup>15,19</sup> which raises the possibility of typically metallic collective excitations, such as itinerant magnetization waves. At least three different competing types of magnetic fluctuations have been predicted<sup>9,13,14,15,16,17</sup> and an ordered spin density wave was first predicted<sup>9,15</sup> and subsequently observed experimentally in the non-superconducting undoped parent, LaFeAsO<sup>10,11,12</sup>. Currently, most researchers agree that superconductivity in this compound is unconventional and likely related to magnetism<sup>15,16,17,18,19,20,21,22,23,24,30,31</sup>.

The uncommon richness of the electronic structure of this compound has already led to a situation in which different theoretical groups report density functional theory (DFT) band structure calculations that emphasize proximity to different magnetic states: weak ferromagnetism<sup>13,14</sup>, checkerboard antiferromagnetism<sup>13,15,17</sup>, an antiferromagnetic stripe phase<sup>9,15</sup>. For the general reader, it may look as if dif-

ferent DFT calculations disagree among themselves and that, beyond a general initial consensus on the commonalities of the different materials, electronic structure calculations differ in details of the ground state and in the band structure near the Fermi level. The reason for such inconsistencies is not just computational inaccuracy, as it may seem, but rather has a physical origin. Namely, as pointed out by a number of authors and discussed in detail below, magnetism in this compound is very itinerant, making the calculated magnetic energies and moments extremely sensitive to the approximation used and to tiny details of the crystal structure. This situation is relatively unusual, particularly in comparison to compounds with localized magnetic moments, which are normally rather robust. Thus, there may be a tendency to ascribe reported differences to an inherent inaccuracy of electronic structure calculations, rather than to the peculiar dependencies of the compound itself. Here we outline those dependencies and provide a reference set of calculations in an attempt to establish a clear theoretical picture within DFT.

There is a kernel of truth underlying the perception that DFT results are disparate: for soft itinerant magnets one has to exercise extra caution in the calculational parameters in order to get consistent and reliable results. In particular, methods that imply restriction on the shape of the charge density (such as Atomic Sphere Approximation) and methods that involve pseudization of the crystal potential can be trusted only after they

have been tested against all-electron, full-potential calculations. Furthermore, in this particular compound the magnetic properties show an unusual sensitivity to the internal As height and are also sensitive, unusual for localized moments but typical for itinerant magnets, to the exchange correlation potential.

Before investigating the magnetic properties and their dependencies in detail, it is important to note that this system is in proximity to a quantum critical point that results in strong spin fluctuations and to establish how such a system is best dealt with theoretically. It is well known (Refs. 32,33 and references therein) that DFT calculations, which are mean-field by nature, underestimate the effect of spin fluctuations that generally depress or suppress long-range magnetic order. It is also understood that gradient corrections (GGA) to the local density approximation generally increase the tendency to magnetism. As a rule of thumb, in systems with strong local Coulomb correlations, such as cuprates or 3d metal oxides, GGA better describes magnetic properties (an even further improved description is provided by the LDA+U method), while in itinerant magnets or near-magnets, LDA is closer to experiment in terms of magnetism. The classical examples are Pd metal and  $\text{Sr}_2\text{RuO}_4$ ; both are ferromagnetic in GGA, but not (in agreement with the experiment) in LDA. On the other hand, GGA is usually better at predicting the crystal structure of transition metal compounds. Finally, given the same crystal structure, the bands themselves are practically indistinguishable whether calculated in LDA or GGA. With these facts in mind, previous experience in first principles DFT calculations suggests that the best approach to the  $\text{LaFeAsO}$  family may be to optimize the structure (if necessary) using GGA and to calculate magnetic properties using LDA (while LDA consistently overestimates the tendency to magnetism compared to the experiment, it always fares better than GGA). Either functional can be used to analyze bands and Fermi surfaces. If a quantitative value of the magnetic stabilization energy is less important than an accurate analysis of a *trend* (say, with doping), GGA may be chosen for the reason that it amplifies the tendency to magnetism and results in larger numbers that are easier to compare with each other. What is important though is that as long one uses full-potential, all-electron methods (or well tested pseudopotentials) the results agree satisfactorily with each other, within the same density functional (LDA or GGA). It is worth noting that one can envision a situation where proper account for the energy associated with magnetic fluctuations may be more important than one-electron excitation spectrum (even when addressing the mechanism of superconductivity). In such a case, spin-polarized GGA may give more insight than LDA (despite yielding an obviously exaggerated magnetic ground state); there is little previous experience to guide band theory procedure in this case.

Let us now discuss the reported results of magnetic calculations in more detail. Three different long range

TABLE I: Magnetic stabilization energies (vs. non-magnetic) and magnetic moments for zero doping and hole ( $x = 0.1$ ) doping in the experimental and optimized structures. Unfilled boxes correspond to unstable (vs. metastable) configurations.

optimized coordinates		$x = 0.0$		$x = 0.1$	
		GGA	LDA	GGA	LDA
$E_{stab}$ (meV)	FM	0.1	0.0	–	–
	AFM (c)	22	–	10	–
	AFM (s)	82	25	64	9
$\mu$ ( $\mu_B/\text{Fe}$ )	FM	0.1	0.1	–	–
	AFM (c)	1.4	–	1.3	–
	AFM (s)	1.8	1.2	1.8	1.0
experimental coordinates		$x = 0.0$		$x = 0.1$	
		GGA	LDA	GGA	LDA
$E_{stab}$ (meV)	FM	5.1	0.7	1.4	0.3
	AFM (c)	87	26	85	28
	AFM (s)	180	84	171	75
$\mu$ ( $\mu_B/\text{Fe}$ )	FM	0.3	0.2	0.2	0.1
	AFM (c)	1.8	1.5	1.8	1.5
	AFM (s)	2.2	1.8	2.2	1.8

magnetic orders in the Fe plane have been so far considered: a ferromagnetic ordering that retains the crystal symmetry  $P4/nmm$  (#129) with two formula units per cell, a checkerboard antiferromagnetism ( $P4m2$ , #115, two formulas), and an antiferromagnetism with alternating stripes along 100 ( $Pccm$ , #49, four formula units). Singh and Du<sup>13</sup>, following the prescription above, presented LDA calculations for the undoped and 10% doped materials. They found, using an in-house full-potential LAPW code, that the undoped material is barely unstable against weak ferromagnetism ( $M \lesssim 0.1\mu_B/\text{Fe}$ ), but stable against checkerboard antiferromagnetism. Similarly, it was found that in LDA the ferromagnetic instability rapidly disappears with doping and at  $x = 0.1$  no longer exists. Mazin *et al*<sup>15</sup> later discovered that within LDA the doped material is unstable against the stripe AFM ordering. It was shown subsequently shown<sup>9</sup> that this is the universal ground state *within DFT* at all dopings including zero.

Soon after, Cao *et al*, using pseudopotential methods, reported GGA results for the checkerboard AFM ordering in the absence of doping. They used two different techniques, VASP+PAW<sup>34</sup> and PW-SCF ultrasoft pseudopotential<sup>35</sup>. Neither of these methods is all-electron and therefore depends on the selected pseudopotential (especially for Fe). Not surprisingly, while qualitative conclusions agree with all-electron calculations, quantitatively they differ both between themselves and with the all-electron “exact” result. Their VASP calculations gave a very large magnetic stabilization energy of 84 meV/Fe, while PW SCF produced 14 meV/Fe.

Similarly, Dong *et al*<sup>9</sup> reported pseudopotential calculations for the stripe ordering proposed in Ref.<sup>15</sup>, also in GGA, and found a stabilization energy of 40 meV/Fe and magnetic moment of  $1.5\mu_B$  (Dong *et al* do not indicate what level of doping they were using, but their plots are

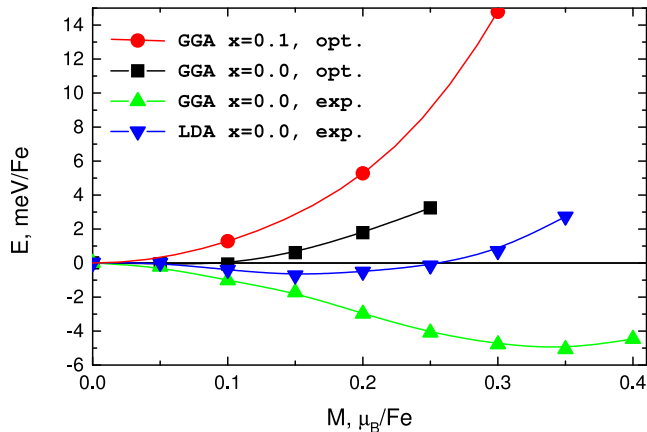


FIG. 1: (color online) Fixed spin moment calculations for  $\text{LaFeAsO}_{1-x}\text{F}_x$ .

consistent with  $x=0.1$ ).

An extensive study of both types of AFM ordering was reported by Yildirim<sup>28</sup> who performed both pseudopotential (which he discarded as unreliable) and all-electron calculations using LDA. Using fixed spin moment calculations, he found that only the stripe order is stable with respect to a non-magnetic state. Ma *et al*<sup>18</sup>, using GGA and a pseudopotential approach, also found the stripe order to be the ground state, but also found a metastable checkerboard AFM state.

Finally, Yin *et al*<sup>29</sup> performed GGA calculations and observed that (a) the magnetic moment depends on the As position anomalously strongly and (b) the As positions, optimized in GGA (as it is generally considered to be the most accurate for the structural properties), differ from the experimentally reported by as much as 0.1 Å, an exceptionally large discrepancy.

With this in mind, we have performed calculations using a variety of codes: two entirely different all electron full-potential codes (WIEN2k<sup>36</sup> and FPLO<sup>37</sup>), as well as two different pseudopotential codes (VASP<sup>34</sup> and PW SCF<sup>35</sup>). The two all-electron codes gave nearly identical results, while the pseudopotential results differed somewhat, though not drastically, both from all-electron and from each other to some degree. We pursued the “standard” route discussed in the earlier section (using GGA for optimization and then recalculating the magnetic properties using LDA). Optimization is performed in the paramagnetic phase, since experimentally these materials are either paramagnetic or have a drastically suppressed magnetic moment of 0.15-0.35  $\mu_B$ . The experimental lattice parameters,  $a = 4.035$  and  $c = 8.741$  Å were used. We also compare our results to those in LDA (in the same structure) and to both LDA and GGA calculations in the experimental structure.

Optimization leads to As and La positions that vary little with doping: from  $z_{\text{La}} = 0.1450$ ,  $z_{\text{As}} = 0.6380$  at

$x = 0$  to  $z_{\text{La}} = 0.1490$ ,  $z_{\text{As}} = 0.6340$  at  $x = 0.2$ . Reported experimental data are, respectively, 0.1415 and 0.6513 at zero doping, and practically the same at  $x = 0.1$  (ref.). As pointed out by Yin<sup>29</sup>, the discrepancy in the As position amounts to 0.1 Å, a nearly unheard-of an error for GGA calculations. In Table I and Fig. 1 we show how the magnetic stabilization energy varies as a function of doping for the optimized and experimental structures. One sees that all GGA results are substantially more magnetic (expectedly) as are the calculations in the experimental structure (unexpectedly). A consistent set of numbers for calculations using all-electron WIEN2k are given, with comparison numbers from other codes also included. The two all-electron methods differ by about 10% in terms of magnetic energy; pseudopotential calculations are somewhat more off, especially the PW SCF. Importantly, all of the them predict the same energy sequence (this is however *not* the case if a pseudopotential without  $p$  states in the valence is chosen for Fe<sup>38</sup>). Finally, we compare the results with published calculations and find the same trend: all electron calculations agree reasonably well among themselves, while pseudopotential ones, being sensitive to the choice of pseudopotential, scatter more.

Interestingly, apart from the structural parameters themselves LDA results obtained using the GGA-optimized structure seem to correspond more closely to what is physically observed than those obtained using the experimental structure. General experience indicates that magnetism in metals near quantum critical points can be entirely suppressed by fluctuations if the LDA magnetic energy is on the order of 10-15 meV per atom, but it is rather hard for spin fluctuations to entirely destroy magnetism that is stabilized by any substantially larger energy. The stabilization energy for the stripe antiferromagnetism in the experimental structure is 75 meV ( $x = 0.1$ ), far too much to expect full suppression of magnetic order from spin fluctuations. In the theoretical structure, on the other hand, the same energy is 9 meV, which is in precisely the range of energies that accumulated knowledge of itinerant magnets indicates can be overcome by spin fluctuations.

The Fermi surfaces corresponding to the GGA-optimized structure in comparison to those of the experimental structure further support use of the optimized structure. An empirical observation can be made that the border between the SDW antiferromagnetism and superconductivity in  $\text{LaFeAsO}_{1-x}\text{F}_x$  is roughly at the same concentration ( $x \sim 0.03$ )<sup>9</sup> where the only substantially 3D piece of the Fermi surface disappears ( $x \sim 0.05$ ). At the same doping level, magnetic ordering disappears, very much in line with standard intuition that long range order in a 2D system is easily destroyed by fluctuations. Superconductivity appears at the same time, suggesting, rather naturally, that at smaller  $x$  it is simply suppressed by the magnetic order. The nice correlation between dimensionality, magnetism, and superconductivity is entirely destroyed in calculations based on the experimen-

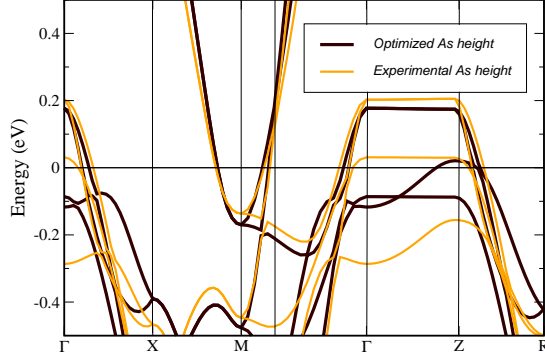


FIG. 2: (color online) A comparison of the band structure derived using experimental coordinates to that using optimized coordinates. The three-dimensional band that crosses the Fermi energy in the optimized structure is extraordinarily sensitive to As height, dropping below  $E_F$  when it is raised to the experimental position. It is replaced by a two-dimensional band.

tal structure. The 3D band that crosses  $E_F$  and forms a small pocket around the Z point of the BZ (see Fig. 2) in the optimized structure is far below  $E_F$  in the experimental structure, replaced by a strongly 2D band. In other words, expanding the Fe-As distance exchanges the positions of a 3D and a 2D band, causing the latter to cross  $E_F$ . The system is then two-dimensional for all values of  $x$  and doping is expected to have little effect on the strength of the spin fluctuations. Of course, at some doping this 2D band will also fill (similar to the 3D band of the optimized structure), but no dimensional crossover will occur coincident with the disappearance of the Fermi surface.

Although the experimental trends can seemingly be better explained by using the GGA-optimized coordinates followed by LDA magnetic calculations than by using GGA magnetic calculations or experimental coordinates, as outlined above, the exception of the coordinates themselves is important. Surprisingly, applying spin polarization *and* the GGA exchange-correlation potential during optimization leads to rather good agreement with experiment for internal positions as well as lattice constants (the latter are already reasonably reproduced in paramagnetic GGA calculations). The Fe-As height, to which the FS and magnetism are unusually sensitive, is obtained as 2.38 Å, acceptably close to the experimentally observed height of 2.41 Å. Thus, there is a contradiction between good agreement in structural parameters and wildly overestimated magnetism (or conversely, good magnetic energies/moments and badly underestimated bond-lengths) that remains one of the more confusing aspects of this compound. In order to fully understand how magnetism manifests itself in this family of materi-

als, which is crucial as a beginning step to understand the relationship between magnetism and superconductivity, the connection between the physical and magnetic structures must be disentangled. This remains an open and intriguing problem.

We now address the origin of the antiferromagnetic interactions. As pointed out in Ref.<sup>15</sup>, all three magnetic instabilities have entirely different physical origins: ferromagnetism is of the Stoner type, checkerboard antiferromagnetism results from the combined effort of conventional superexchange and of nesting of two electron pockets<sup>39</sup>, while the stripe ordering appears because of nesting between the hole and electron pockets, and is additionally supported<sup>28</sup> by the next-n.n. superexchange. It has been assumed by some authors<sup>28,30,31,40</sup> that superexchange is the leading cause of both AFM instabilities, and, by implication, that a two-shell Heisenberg model provides a meaningful description of magnetism. Others<sup>9,15,19</sup> emphasized the long-range character of magnetic interaction, coming from interband spin susceptibility. The physical difference between the two descriptions is enormous: the former implies AFM in real space, that is, each two individual ions that are neighbors or next neighbors to each other interact antiferromagnetically, but there is no direct interaction at longer distances. The latter interaction is local in the reciprocal space, that is, it corresponds to condensation of a spin-density wave (even though only a *finite* amplitude SDW is stable), and requires ordering on the scale of at least several unit cells to exhibit antiferromagnetism. Direct evidence in favor of the long-range SDW scenario comes from the calculations of Yin *et al.*<sup>29</sup>: they have computed nn and nnn exchange constant in the ordered stripe phase *with respect to the small deviations from the AFM ordering*. They found that the exchange constants have opposite signs along the CDW wave vector and in the perpendicular direction. Given that the underlying structure is tetragonal and the x/y asymmetry arises entirely due to the magnetic ordering itself, this proves beyond any doubt that the Heisenberg Hamiltonian is not applicable for this system.

We have also undertaken a more conventional test that also confirms the SDW character of the stripe antiferromagnetism. First, one can try to map the magnetic energy of the two stable AFM structures onto the n.n. Heisenberg model. This is a routine procedure for localized systems. Here, however, it has the problem that the moments are so soft that not all desired magnetic patterns can be realized, most notably the FM structure, and different patterns converge to different magnetic moment amplitudes (extreme softness of the magnetic moment magnitude already implies that the application of the Heisenberg Hamiltonian is suspect). This problem was realized by Yildirim who added an external field (when needed, staggered) to converge all three patterns he considered at the same moment magnitudes. The hope is that the result is not too sensitive to the shape of the staggered field (which is true for localized



moments, but not necessarily for itinerant ones). Ma, on the other hand, allowed the moments to vary freely within each of the three antiferromagnetic orderings, and found magnetic moments ranging from 2.2 - 2.6  $\mu_B$ , and then adjusted the ferromagnetic structure to have approximately the same moment.

In the checkerboard structure, the Heisenberg (or Ising, in this case) exchange energy per site,  $\sum_{i>j} J_{ij} M_i M_j$ , is  $E_{cb} = -2(J_{nn} - J_{nnn})M^2$ , and in the stripe phase  $E_{st} = -2J_{nnn}M^2$  (with respect to the non-magnetic state). It is also possible<sup>40</sup> to stabilize an intermediate magnetic structure, where the sites with the coordinates  $(2n, 2m)$  have spins up,  $(2n + 1, 2m + 1)$  spins down, and  $(2n + 1, 2)$  and  $(2n, 2m + 1)$  are not magnetic. In that case the magnetic energy per site is half that of the stripe phase,  $-J_{nnn}M^2$ . Finally, the ferromagnetic state energy in the Heisenberg model is  $+2(J_{nn} + J_{nnn})M^2$ . Ma *et al*<sup>40</sup> give for the ferromagnetic, checkerboard, stripe and the intermediate structures the energies of +91, -217, -109 and -65 meV/Fe, respectively. It is obvious that these four numbers are nowhere close to be mappable onto this model, contrary to the claim in Ref.<sup>40</sup>. It is also worth noting that the very fact that the checkerboard structure is stable in GGA implies  $J_{nn} > J_{nnn}$ , contrary to the popular belief<sup>30,31</sup> that the nnn superexchange is stronger here.

One may notice that the energies above are inconsistent with any published all-electron calculation, so one may agree with Yildirim<sup>28</sup> that in this case pseudopotential calculations cannot be trusted (although our own experience indicates that *carefully and properly selected* pseudopotentials are still reasonable). To test that, we have performed similar calculations using the all-electron WIEN code, also using the optimized structure,  $x = 0$  and GGA (which makes sense in this particular case in order to artificially emphasize the magnetism). We found the four energies in question to be +166, -18, -81 meV and -36 meV (and the moments ranging from 1.5 to 1.8  $\mu_B$ ). These numbers are reliable DFT results, with no uncontrollable approximations such as pseudization of the potentials, yet they are just as incompatible with the two-neighbor Heisenberg model as are Ma *et al*'s results, in agreement with the perturbative calculations of Yin *et al*.

We conclude this section by restating the main points relevant to magnetic calculations in this system. In both GGA and LDA the undoped system is on the verge (within a fraction of a meV) of an instability against an itinerant ferromagnetic state with a very small magnetic moment. The AFM checkerboard structure, reminiscent of the magnetic ordering of Cu planes in cuprates, is quite stable, albeit not the ground state, in both LDA and GGA, if one uses experimental As positions, in either the doped or undoped compounds. In the optimized structure the checkerboard magnetism is stable only in GGA, and by a rather small energy. The striped structure is the DFT ground state for all relevant dopings, independent of the As position; in GGA it is very sta-

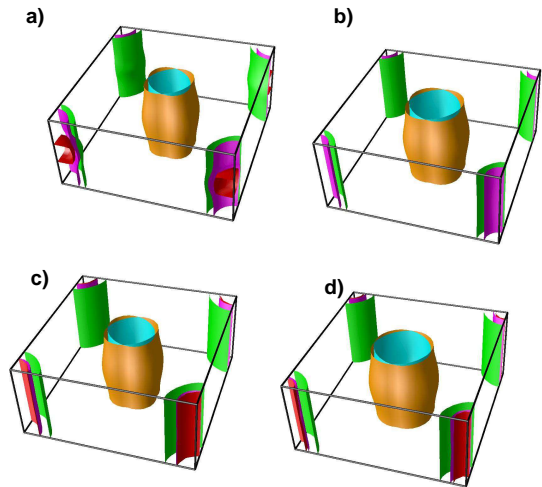


FIG. 3: (color online) GGA Fermi surfaces of  $\text{LaFeAsO}_{1-x}\text{F}_x$ , for a)  $x=0$  with optimized coordinates, b)  $x=0.1$  with optimized coordinates, c)  $x=0$  with experimental coordinates, and d)  $x=0.1$  with experimental coordinates. Note that the band structure is three dimensional at low doping in the optimized structure, but becomes two-dimensional with doping, while in the experimental structure it is two-dimensional and insensitive to doping

ble, while in the LDA, and if one uses optimized positions, it rapidly becomes a borderline instability that can be easily destroyed by fluctuations, in agreement with the experiment. Magnetism cannot be described, not even qualitatively, using two superexchange coupling constants, not even if one adds a Stoner energy reflecting the softness of individual spins. Only LDA calculations, and only in the optimized structure, provide a quantitatively realistic picture of the magnetic properties of this system in the entire doping range. It is worth reiterating that in borderline magnets, of which this system is clearly an example, not only is LDA closer to experiment than GGA, but in real materials fluctuations suppress magnetism even further, so that in comparison to GGA, LDA is a step in the right direction, but does not go the whole way.

In the second part of this work, we concentrate on a detail of the Fermi surface that is crucially important for some of the proposed superconductivity theories, as well as for some of the magnetic orderings: the eccentricity of the overlapping ellipses around the  $M$  point of the BZ. The importance of the eccentricity is obvious from the fact that if the electron pockets were ideal circles (though they do not have to be, by symmetry), just as the hole pockets, they would nest ideally with each other, creating a sharp nesting peak at  $Q = \pi, \pi$  and strongly enhancing the tendency to checkerboard AFM ordering. At the particular doping where the number of holes is exactly equal to the number of electrons, the hole and the electron pockets would also nest ideally, making this specific concentration very special from the electronic point

TABLE II: Calculated eccentricities,  $e(\Gamma)$  and  $e(Z)$  of the electron Fermi surfaces as a function of doping level with different methods. Here  $e(\Gamma)$  and  $e(Z)$  are in the  $k_z=0$  and  $k_z=0.5$  planes, respectively. Note that at low doping there is an additional 3D hole sheet.

		$e(\Gamma)$	$e(Z)$
FP	$x=0$	0.34	0.59
(Wien)	$x=0.1$	0.26	0.48
FP	$x=0$	0.31	0.61
(FPLO)	$x=0.1$	0.23	0.48
PAW	$x=0$	0.28	0.52
(VASP)	$x=0.1$	0.18	0.42
PP	$x=0$	0.20	0.48
(PWSCF)	$x=0.1$	0.15	0.42
PP <sup>19</sup>	$x=0$	0.20	
PP <sup>21</sup>	$x=0$	0.09	0.42
	$x=0.1$	0.0	
PP <sup>17</sup>	$x=0$	0.26	

of view. In addition, such sharp structure in the magnetic susceptibility is favorable for exotic order parameter distributions with nodes, set not by symmetry but by resonance effects between the peaks in the susceptibility and the Fermi surface geometry<sup>19</sup>. At least one of the proposed theories<sup>20,21</sup> relies on the condition that two rotated electron pockets coincide with an accuracy in energy not worse than the superconducting gap.

Although the band structure and fermiology are much less sensitive to calculational method than the stabilization energies are, there is still some variation between methodologies and substantial differences occur between published reports (in the latter case, largely due to variance among the structures used by different authors).

We have summarized our own results, again using two all electron full-potential codes and two pseudopotential codes in Table II, where we additionally include eccentricities extracted from other reported calculations. The eccentricity in the  $\Gamma-X-M$  ( $k_z=0$ ) plane is listed, and, where available, in the  $Z-R-A$  plane ( $k_z=0.5$ ). The latter is universally larger, due to the fact that the longer axis of the ellipse is formed by the only band around the M point that is (somewhat)  $z$ -dispersive.

Again we see excellent (nearly perfect) agreement between our two all electron results with more deviation in the pseudopotential ones. In fact, all pseudopotential calculations appear to underestimate the eccentricity, some by a large amount. Ref. 21 has reported zero eccentricity at a doping of  $\sim 10\%$  in the  $\Gamma$  plane, far less than not only both all-electron calculations, but also other pseudopotential results. Surprisingly, in the  $Z$  plane, the eccentricity very closely matches our pseudopotential results, indicating a highly dispersive band absent from our calculations. This is in some sense unfortunate, because a very interesting model of interband *triplet*  $s$ -wave pairing<sup>20</sup> is only viable if the energy difference between the two bands at the M point is smaller near the point where they cross the Fermi level, than the superconduct-

ing gap. Our all-electron results unequivocally indicate that this difference is at least 100 meV in the  $k_z=0$  plane and at least 180 meV in the  $k_z=\pi/c$  plane.

Several things should be noted when comparing these calculations. The first is that doping is accounted for differently in our pseudopotential calculations than in our all-electron calculations. In the former, the desired number of electrons are added and compensated for with a uniform positive background. In the latter, electron doping is obtained using a fictitious O atom with increased core charge and electrons and hole doping is obtained using a fictitious La atoms with decreased core charge and electrons. Thus, one should not expect the two different methodologies to produce identical results. The second thing is that for calculations other than our own in Table II, different lattice constants or internal coordinates may have been employed, although it is our experience that, within reasonable limits, these never drastically reduce the eccentricities (even though the actual numbers change).

In conclusion, we show that while the magnetic ground state of  $\text{LaFeAsO}_{1-x}\text{F}_x$  can be obtained using any of several methodologies (all-electron, pseudopotential with ultra-soft or pseudopotential with PAW), the details of the magnetic properties, such as site magnetization and magnetic energy differences may be affected by pseudization of the crystal potential. More importantly, the results depend drastically on the exchange-correlation functional used (GGA vs. LDA) and on the position of As. The best results in terms of explaining the observed magnetic phase diagram are obtained within LDA (which is the recommended functional for itinerant magnets) and using the theoretical As positions. The fermiology and band structure are less sensitive to the details of the calculation, with the three all-electron codes we applied giving identical results. Small Fermi surface details, such as the eccentricity of the central ellipses, differed between all-electron and pseudopotential codes and between different pseudopotential codes, though a careful application of the latter yielded results that differ only slightly from the all-electron results. We have reported a reference set of calculations for the basic electronic structure properties of the parent compound and for several dopings (both hole and electron). We believe these will provide a consistent and accurate basis of knowledge upon which models and theories about this interesting compound can be built.

## Acknowledgments

Work at NRL was supported by the Office of Naval Research. Work at ORNL was supported by the Department of Energy, BES, Division of Materials Sciences and Engineering.

*Note added in proof:* After submission of this manuscript, we became aware of a paper by Ishibashi *et*.

$at^{41}$ . These authors applied an in-house pseudopotential code to four different fully AFM patterns ( $\mu \geq 1.8 \mu_B$  on all sites). Their stabilization energies in all four cases agree with our all-electron results within 7 meV/formula unit. Curiously, if one discards the FM pattern, the three

energy differences among the remaining AFM states can be fitted with a two-parameter Heisenberg model fairly well. However, the fact that the FM ordering does not fit into this picture at all suggests that the fit is fortuitous.

- 
- <sup>1</sup> Y. Kamihara, T. Watanabe, M. Hirano, and H. Hosono, J. Am. Chem. Soc. **130**, 3296 (2008).
  - <sup>2</sup> Z.A. Ren, J. Yang, W. Yi, G.C. Che, X.L. Dong, L.L. Sun, Z.X. Zhao, arXiv:0803.4283 (2008).
  - <sup>3</sup> G.F. Chen, Z. Li, G. Li, J. Zhou, D. Wu, J. Dong, W.Z. Hu, P. Zheng, Z.J. Chen, J.L. Luo, and N.L. Wang, arXiv:0803.0128 (2008).
  - <sup>4</sup> A.S. Sefat, M.A. McGuire, B.C. Sales, R. Jin, J.Y. Howe, and D. Mandrus, arXiv:0803.2528 (2008).
  - <sup>5</sup> G.F. Chen, Z. Li, D. Wu, G. Li, W.Z. Hu, J. Dong, P. Zheng, J.L. Luo, and N.L. Wang, arXiv:0803.3790 (2008).
  - <sup>6</sup> P. Cheng, L. Fang, H. Yang, X. Zhu, G. Mu, H. Luo, Z. Wang, and H.H. Wen, arXiv:0804.0835 (2008).
  - <sup>7</sup> X.H. Chen, T. Wu, G. Wu, R.H. Lin, H. Chen, and D.F. Fang, arXiv:0803.3603 (2008).
  - <sup>8</sup> G.F. Chen, Z. Li, D. Wu, J. Dong, G. Li, W.Z. Hu, P. Zheng, J.L. Luo, and N.L. Wang, arXiv:0803.4384 (2008).
  - <sup>9</sup> J. Dong, H.J. Zhang, G. Xu, Z. Li, G. Li, W.Z. Hu, D. Wu, G.F. Chen, X. Dai, J.L. Luo, Z. Fang, and N.L. Wang, arXiv:0803.3426 (2008).
  - <sup>10</sup> Z.W. Zhu, Z.A. Xu, X. Lin, G.H. Cao, C.M. Feng, G.F. Chen, Z. Li, J.L. Luo, and N.L. Wang, arXiv:0804.1324 (2008).
  - <sup>11</sup> C. de la Cruz, Q. Huang, J.W. Lynn, J. Li, W. Ratcliff II, J.L. Zarestky, H.A. Mook, G.F. Chen, J.L. Luo, N.L. Wang, and P. Dai, arXiv:0804.0795 (2008).
  - <sup>12</sup> M.A. McGuire, A.D. Christianson, A.S. Sefat, R. Jin, E.A. Payzant, B.C. Sales, M.D. Lumsden, and D. Mandrus, arXiv:0804.0796 (2008).
  - <sup>13</sup> D.J. Singh and M.H. Du, arXiv:0803.0429 (2008).
  - <sup>14</sup> K. Haule, J.H. Shim, and G. Kotliar, arXiv:0803.1279 (2008).
  - <sup>15</sup> I.I. Mazin, D.J. Singh, M.D. Johannes, and M.H. Du, arXiv:0803.2740 (2008).
  - <sup>16</sup> G. Xu, W. Ming, Y. Yao, X. Dai, S.C. Zhang, and Z. Fang, arXiv:0803.1282 (2008).
  - <sup>17</sup> C. Cao, P.J. Hirschfeld, and H.P. Cheng, arXiv:0803.3236 (2008).
  - <sup>18</sup> F. Ma, and Z.Y. Lu, arXiv:0803.3286 (2008).
  - <sup>19</sup> K. Kuroki, S. Onari, R. Arita, H. Usui, Y. Tanaka, H. Kontani, and H. Aoki, arXiv:0803.3325 (2008).
  - <sup>20</sup> X. Dai, Z. Fang, Y. Zhou, and F.C. Zhang, arXiv:0803.3982 (2008).
  - <sup>21</sup> H.J. Zhang, G. Xu, X. Dai, and Z. Fang, arXiv:0803.4487 (2008).
  - <sup>22</sup> Q. Han, Y. Chan, and Z.D. Wang, arXiv:0803.4346 (2008).
  - <sup>23</sup> L. Boeri, O.V. Dolgov, and A.A. Golubov, arXiv:0803.2703 (2008).
  - <sup>24</sup> P.A. Lee and X.G. Wen, arXiv:0804.1739 (2008).
  - <sup>25</sup> I.A. Nekrasov, Z.V. Pchelkina, and M.V. Sadovskii, arXiv:0804.1239 (2008).
  - <sup>26</sup> S. Raghu, X.-L. Qi, C.-X. Liu, D. Scalapino, and S.-C. Zhang, arXiv:0804.1113 (2008).
  - <sup>27</sup> S. Graser, G.R. Boyd, C. Cao, H.-P. Cheng, P.J. Hirschfeld, and D.J. Scalapino, arXiv:0804.0887 (2008).
  - <sup>28</sup> T. Yildirim, arXiv:0804.2252 (2008).
  - <sup>29</sup> Z. P. Yin, S. Lebegue, M. J. Han, B. Neal, S. Y. Savrasov, W. E. Pickett, arXiv:0804.3355 (2008).
  - <sup>30</sup> Q. Si, E. Abrahams, arXiv:0804.2480 (2008).
  - <sup>31</sup> C. Fang, H. Yao, W.-F. Tsai, J. Hu, S. A. Kivelson, arXiv:0804.3843 (2008).
  - <sup>32</sup> P. Larson, I.I. Mazin, D.J. Singh, Phys. Rev. **B69**, 064429 (2004).
  - <sup>33</sup> *Density Functional Calculations near Ferromagnetic Quantum Critical Points*, I. I. Mazin, D.J. Singh, and A. Aguayo, in *Proceedings of the NATO ARW on Physics of Spin in Solids: Materials, Methods and Applications*, ed. S. Halilov, Kluwer, 2004.
  - <sup>34</sup> G. Kresse and J. Furthmüller, Phys. Rev. B **54**, 11169 (1996) and G. Kresse and D. Joubert, Phys. Rev. B **59**, 1758 (1999).
  - <sup>35</sup> S. Baroni, A. Dal Corso, S. de Gironcoli, P. Giannozzi, C. Cavazzoni, G. Ballabio, S. Scandolo, G. Chiarotti, P. Focher, A. Pasquarello, K. Laasonen, A. Trave, R. Car, N. Marzari, and A. Kokalj, <http://www.quantum-espresso.org>
  - <sup>36</sup> P. Blaha, K. Schwarz, G.K.H. Madsen, D. Kvasnicka, and J. Luitz, WIEN2K, An augmented planewave+local orbitals program for calculating crystal properties (Technische Universität Wien, 2002, Austria); <http://www.wien2k.at>
  - <sup>37</sup> K. Koepernik and H. Eschrig, Phys. Rev. B **59**, 1743 (1999); I. Opahle, K. Koepernik, and H. Eschrig, Phys. Rev. B **60**, 14035 (1999); <http://www.fplo.de>
  - <sup>38</sup> The AFM checkerboard configuration is unstable against a non-magnetic state for pseudopotentials with p states in the core. Furthermore, the older Perdew-Wang (1991) parameterization also finds a non-magnetic ground state. Only the Perdew-Burke-Ernzerhof parameterization with p states in the valence correctly reproduces the magnetic ground state found using all-electron methods.
  - <sup>39</sup> Here and below we use the word “nesting” in a loose way, applying it to any interaction derived from lowering energy by removing one-electron states from the Fermi level. It is important to realize that the peaks in the calculated one-electron susceptibility are not sharp enough to induce instability with respect to an infinitesimally small perturbation with the “nesting” wave vector, whether for the stripes or for the checkerboard structure. The instability occurs only for SDWs of large amplitudes, in which case the perfect nesting exactly at the Fermi level is less important.
  - <sup>40</sup> F. Ma, Z.Y. Lu, and T. Xiang, arXiv:0803.3370 (2008).
  - <sup>41</sup> S. Ishibashi, K. Terakura, and H. Hosono, J. Phys. Soc. Japan **77**, 053709 (2008).